

PAPER • OPEN ACCESS

Design and Analysis of a Self-balancing Bicycle Model

To cite this article: G Nitheesh kumar *et al* 2021 *IOP Conf. Ser.: Mater. Sci. Eng.* **1132** 012014

View the [article online](#) for updates and enhancements.

You may also like

- [Absorption modulation of quasi-BIC in Si-VO₂ composite metasurface at near-infrared wavelength](#)
Hongxiang Dai, Jukun Liu, Jiaqi Ju et al.
- [Manipulation of the multiple bound states in the continuum and slow light effect in the all-dielectric metasurface](#)
Suxia Xie, Siyi Sun, Zhijian Li et al.
- [Enhancing single photon emission through quasi-bound states in the continuum of monolithic hexagonal boron nitride metasurface](#)
Shun Cao, Yi Jin, Hongguang Dong et al.



UNITED THROUGH SCIENCE & TECHNOLOGY

 The Electrochemical Society
Advancing solid state & electrochemical science & technology

**248th
ECS Meeting**
Chicago, IL
October 12-16, 2025
Hilton Chicago

**Science +
Technology +
YOU!**



**Register by
September 22
to save \$\$**

REGISTER NOW

Design and Analysis of a Self-balancing Bicycle Model

Nitheesh kumar G^{1,*}, Navneeth S¹, Suraj A¹, and Pramod Sreedharan¹

¹ Department of mechanical engineering, Amrita Vishwa Vidyapeetham, Amritapuri, India

* E-mail: nitheeshkumar.g@gmail.com

Abstract. This paper discusses the design and analysis of a self-balancing bicycle model. The objective was to develop an efficient design that can be fabricated in the future. The different methods of balancing a bicycle were studied to develop an optimal design. Solidworks 17 and Ansys 18 have been used for modeling, simulation, and analysis of the structure. The use of a Control Moment Gyroscope (CMG) to balance the bicycle model was studied and the results show that the effect of precession increases with an increase in rpm and the weight of the flywheel. Thus, a bicycle model actuated with CMG is far more stable and less prone to accidental tilts and toppling than one without. The studied data can be used for future research.

1. Introduction

With the evolution of mankind, safety has become a necessity over luxury and comfort in this fast-moving world of transportation. And the implementation of safety in motorcycling always stayed a challenge. Recent studies [1, 2] show that most MTW (Motorized Two-Wheeler) accidents are caused by instability of the vehicle, increasing through the decades, and only an efficiently designed self-balancing two-wheeler can decrease this trend. Moreover, facilitating the commute and recreation of the physically disabled community [3], by efficiently balancing a two-wheeler, was found in demand. Thus, studied the different methods to balance a bicycle with the less human intervention [4].

From further research, it was concluded that CMG can efficiently serve the purpose of balancing a bicycle [4, 5]. CMG is an attitude control device generally used in spacecraft attitude control systems [6]. It consists of a spinning rotor, attached to two gimbals, producing large constant angular momentum. The vector direction of angular momentum can be changed for a two-wheeler by rotating the spinning rotor. A gyroscopic reaction torque orthogonal to both rotor spin and gimbal axes is produced as a result of precession torque applied by the spinning rotor. It amplifies torque because a small gimbal torque input produces a large control torque to the two-wheeler. This method can provide a large torque even though the energy consumption of CMG is very high (as the flywheel is spinning all the time).

For an efficient and manufacturable design, mathematical modeling and design calculations play a major role [7]. Recently, several automobile manufacturing giants have come up with self-balancing technology in their two-wheelers [8] to assist the new era of mankind.

As an initial step to the development of a self-balancing two-wheeler, studied the various parameters that effect the balance of the bike due to the influence of CMG in the system using Solidworks and portrayed the analysis related to its development using Ansys software.



2. System Description

The project was initiated with a 2D sketch of the prototype which then helped to develop a 3D model of the same by using Solidworks. The development of the 3D model was succeeded by the finite element analysis of the individual components using Ansys software. The design was dynamically analyzed using motion analysis in Solidworks. Further, the static analysis of the components verified the structural rigidity for manufacturability. The result of the work was obtained as graphs from the motion analysis.

The main objective was to study the self-balancing nature of a two-wheeler aided with a CMG. Thus, studied the effects of the speed of rotation of the flywheel (part of CMG) on a two-wheeler, with a finite moment of inertia and the time it takes for the setup to completely topple (horizontal to the ground).

3. Mathematical Modelling

Concepts and Formulae:

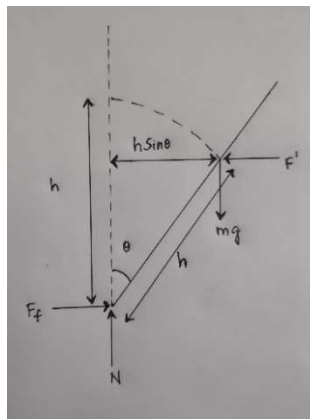


Figure 1. Forces on a self-balancing bicycle

According to 'Figure 1', the mass of the system is m kg, distance/location of the center of mass (m) from the ground is h (m). When the angle of tilt is θ , then the torque induced τ is given by

$$\tau = m g h \sin \theta \quad (1)$$

and the Reactive Gyroscopic Torque (τ') given as

$$\tau' = m g h \sin \theta \text{ (opposite direction)} \quad (2)$$

also,

$$\tau' = I \omega \omega p \quad (3)$$

where I is the moment of inertia of the disc, ω the angular speed of the disc, and ωp the precession speed of the disc.

On comparing equation (2) and equation (3),

$$m g h \sin \theta = I \omega \omega p \quad (4)$$

Therefore,

$$\omega p = m g h \sin \theta / I \omega \quad (5)$$

It is known that maximum frictional force can be written as

$$F'_{\max} = \mu N = \mu m g \quad (6)$$

Where μ is the coefficient of friction and N the normal reaction force.

Hence, at Limiting Condition

$$m g h \sin \theta = F' h \cos \theta \quad (7)$$

on comparing equation (6) and equation (7), the result is

$$m g h \sin \theta = \mu m g h \cos \theta \quad (8)$$

Therefore,

$$\mu = \tan\theta \quad (9)$$

where μ is the coefficient of friction and θ the angle of tilt produced.

The following values are taken from real-world objects available in the market for the best result in the simulation and also for better manufacturability.

Mass of DC motor = 1.06 kg

Mass of battery (12v) = 1.3 kg

Mass of wheels (10'') = 0.8 kg

Mass of Flywheel Disc = 4.165 kg

Mass of Frame = 2.504 kg

Mass of chassis = 2.3 kg

Miscellaneous mass (Nuts, bolts, etc) = 1.1 kg

Total mass = 1.06+1.3+0.8+4.165+2.504+2.3+1.1 = 13.234 kg

$$\begin{aligned} \text{Centre of Mass (CM) from the ground, } h = & [(CM_{\text{wheel}} * M_{\text{wheel}}) + (CM_{\text{chassis}} * M_{\text{chassis}}) + \\ & (CM_{\text{frame}} * M_{\text{frame}}) + (CM_{\text{disc}} * M_{\text{disc}}) + (CM_{\text{hub motor}} * M_{\text{hub motor}}) + (CM_{\text{battery}} * \\ & M_{\text{battery}}) + (CM_{\text{linkage}} * M_{\text{linkage}})] / \text{Total Mass} \end{aligned} \quad (10)$$

Where CM = Centre of Mass

Calculation of center of mass,

$$\begin{aligned} \text{Centre of mass from the ground, } (h) = & (12.7*0.81) + (25.2*2.3) + (30.7*2.3) + (27.2*4.16) \\ & + (18.8*1.06) + (1.3*40.7) + (1.1*18.8) / 13.234 \\ & = 26.087 \text{ cm} \\ & = 0.26087 \text{ m} \end{aligned}$$

Moment of inertia of the disc (I) can be written as

$$I = mr^2 / 2 \quad (11)$$

Where m is the mass of the flywheel and r the radius of the flywheel. Hence

$$\begin{aligned} & = 4.16*(0.075*0.075)/2 \\ & = 0.0117 \text{ kg/m}^2 \end{aligned}$$

The simulation was carried out with a variety of RPMs for comparison. Used rpm value '3350', based on a motor commonly available in the market.

Speed of disc, $N = 3350$ rpm and so, the Angular Speed of Disc, $\omega = 350.81$ rad/sec.

The disc mentioned here is the flywheel (part of CMG), which was initially planned to manufacture in-house. But later on, decided to go with the most easily available and commercially viable option.

The vehicle is designed for the maximum tilt angle equal to 30° .

Therefore, the highest precision speed of the disc, as in equation (5), is

$$\begin{aligned} \omega p & = mgh \sin\theta / I\omega \\ & = 13.234*9.81*0.26*\sin(30) / 0.0117*350.811 \\ & = 4.11 \text{ rad/sec} \end{aligned}$$

And the highest gyroscopic reaction torque, as in equation (3), is

$$\begin{aligned} \tau' & = I\omega\omega p \\ & = 0.0117*350.81*3.479 \\ & = 16.85 \text{ Nm} \end{aligned}$$

4. Design

4.1. Assembly drawing

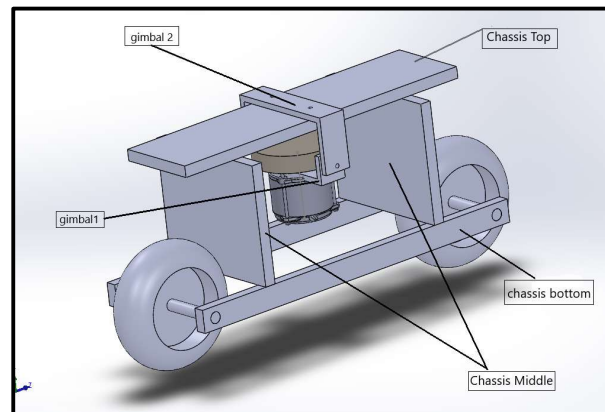
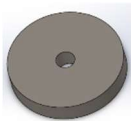
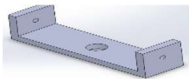



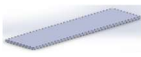





Figure 2. Assembly Drawing of the Prototype

First, a free body diagram in pen and paper was made. It involved many iterations with minimalism and sleek design as a target. The 2D image was first drawn in CAD, and then the part and assembly drawing in Solidworks 'Figure 2'. Detailed descriptions of all Solidworks parts are given in 'Table 1'.

Table 1. Details of Solidworks part drawings

Sl. No	Part	Part Description
1		Flywheel. A disc-shaped solid piece of mild steel with a bore at its geometric center. This is an essential part of the CMG as its rotation helps to maintain the gyroscopic effect needed to keep the two-wheeler's balance.
2		Gimbal 1. This part made of mild steel is necessary to give the second axis of the gyroscope the required free movement to facilitate the production of precession force.
3		Gimbal 2. This part attaches the whole gyroscope to the main chassis, giving the CMG its second axis. This is also made of mild steel.
4		Shaft. It connects the flywheel to the motor. Helps retain the rotation. This is made of mild steel.
5		Motor. A DC motor of maximum speed 3000 rpm. The speed and acceleration of the motor can be controlled using Arduino.
6		Chassis Top. A well-sized plank made of wood makes the top portion of the prototype chassis. The gyroscope is connected to this.
7		Chassis Middle. The plate that makes up the middle portion of the chassis. It is also made up of wood to reduce the weight and also for the ease of manufacturability.
8		Chassis Bottom. The plank makes up the lowest portion or base of the chassis. The middle chassis and the wheels are connected to this part.
9		Wheels. The wheels of desired size 10 inches. This can be purchased from a regular retailer in the market.

5. Results and discussion

5.1. Static Analysis

To test the strength of the materials under static load, the finite element method analysis of all the chassis components was done. It helped to understand the limitations of the designed chassis based on stress and buckling. The intention of this was to understand the amount of load and weight that each component can withstand individually, so as it can be manufactured efficiently. These 'Table 2' and 'Table 3' are the properties we considered for our FEM analysis models in Ansys Software.

Table 2. FEM wood properties [9]

WOOD			
Sl. No	Property	Value	Unit
1	Density	0.56	g cm^{-3}
2	Young's Modulus	6963	MPa
3	Poisson's Ratio	0.415	
4	Bulk Modulus	1.3653 e^{10}	Pa
5	Shear Modulus	2.4604 e^9	Pa
6	Tensile ultimate Strength	31	MPa

Table 3. FEM Mild steel properties

MILD STEEL			
Sl. No	Property	Value	Unit
1	Density	7.85	g cm^{-3}
2	Young's Modulus	2.1 e^5	MPa
3	Poisson's Ratio	0.303	
4	Bulk Modulus	1.7766 e^{11}	Pa
5	Shear Modulus	8.0583 e^{10}	Pa
6	Tensile ultimate Strength	31	MPa

5.1.1. PART 1: Gimbal 1. These models 'Figure 3' and 'Figure 4' represent the total deformation and equivalent stress distribution of the gimbal that is under the direct load of the motor and flywheel. These simulations are magnified to a significant factor (4.1 e^3) to show the deformation.

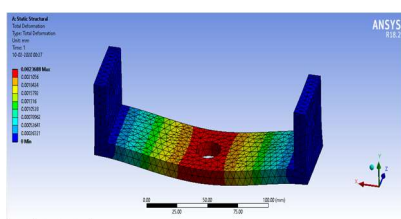


Figure 3. Gimbal 1- Total Deformation

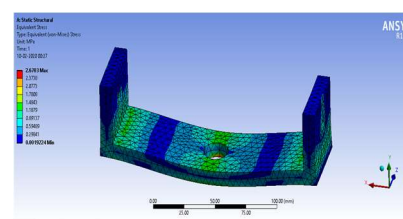


Figure 4. Gimbal 1 - Equivalent Stress

5.1.2. PART 2: Gimbal 2. This gimbal 'Figure 5' and 'Figure 6' supports the weight of the motor, flywheel, and gimbal-1. It is supported at the bottom surface by the 'chassis top' portion.

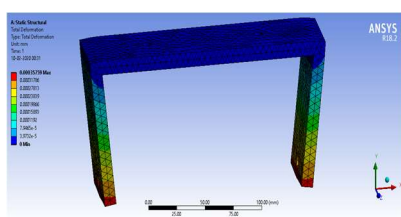


Figure 5. Gimbal 2 - Total Deformation

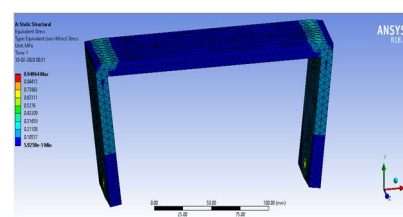


Figure 6. Gimbal 2 - Equivalent Stress

5.1.3. PART 3: Chassis Top. This is the top portion of the chassis, supporting both the gimbals. Wood being the material used, especially considered the forces, stress, and deformation that this may undergo. FEM results, ‘Figure 7’ and ‘Figure 8’, reconfirmed the ability of pre-determined dimensions to support the components.

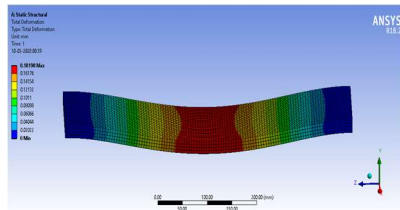


Figure 7. Chassis Top - Total Deformation

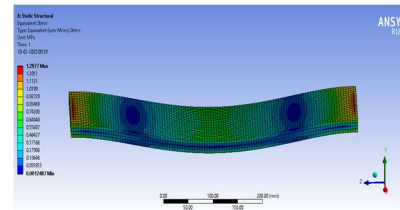


Figure 8. Chassis Top - Equivalent Stress

5.1.4. PART 4: Chassis middle. This, ‘Figure 9’ and ‘Figure 10’, the plywood component that occupies the front and back of the chassis, is not under much force as each of these experiences only half of the total force acted upon by the ‘Chassis Top’ of the body.

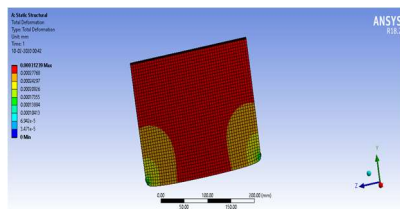


Figure 9. Chassis Middle - Total Deformation

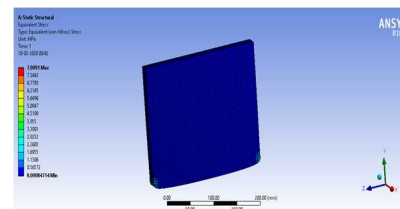


Figure 10. Chassis middle - Equivalent Stress

5.1.5. PART 5: Chassis Bottom. The bottom chassis components ‘Figure 11’ and ‘Figure 12’ are connected to the wheels and also support the entirety of the chassis forces. So, the thickness and rigidity of this component were always under scrutiny. But here too, the FEM analysis shows that the pre-determined dimensions are well within the ability to hold the prototype together.

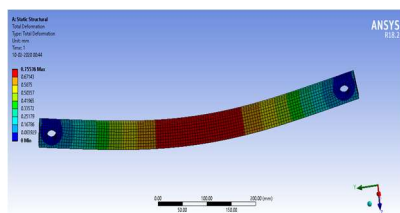


Figure 11. Chassis Bottom - Total Deformation

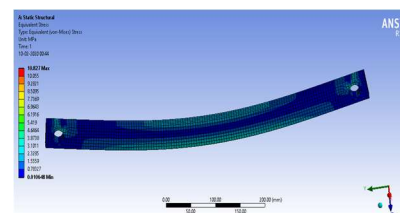


Figure 12. Chassis Bottom - Equivalent Stress

5.1.6. Analysis Result. From the analysis, the maximum amount of distortion that the part undergoes (in mm), the maximum stress formed (in MPa) under the effects of applied forces, support force, and from its weight were found ‘Table 4’. Also given a considerable amount of extra force for a decent margin of safety in the analysis.

Table 4. FEM analysis result

Part	Maximum Deflection (in mm)	Maximum Stress (in MPa)
Gimbal 1	0.00236800	2.67030
Gimbal 2	0.00035759	0.94964
Chassis Top	0.18198000	1.29770
Chassis Middle	0.00031239	7.90910
Chassis Bottom	0.75536000	10.82700

5.2. Dynamic Analysis

The simulation of the prototype in Solidworks 'Figure 13' and 'Figure 14' gave a rough picture of how the prototype will work in real life. The motion analysis also gave the option to try out various scenarios in the prototype design such as using constant and varying rpm, with and without external force, fixed and loose gimbal axes, and many more. Each of these scenarios can be an individual project on its own. The main focus was on knowing and establishing the effect of a working gyroscope in a two-wheeler model.

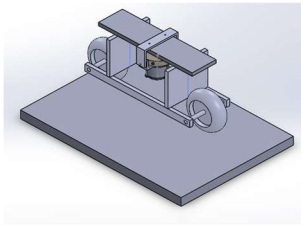


Figure 13. Model orientation at 0 seconds

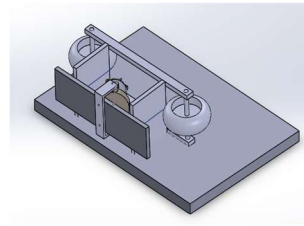


Figure 14. Model orientation at 3.2 seconds

5.2.1. Case 1: Stationary Flywheel (0 rpm). This case is to establish and analytically study the normal day two-wheelers which do not have a gyroscope with them. This Tilt vs Time graph 'Figure 15' clearly shows the time taken to fall from 90 to 0 degrees is about 1.28 seconds.

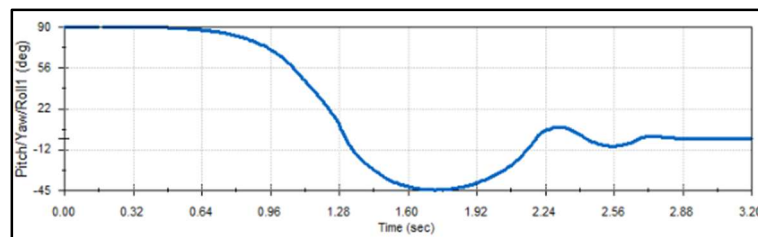


Figure 15. Tilt vs Time (0 rpm)

5.2.2. Case 2: Flywheel at 1000 rpm. When the flywheel is in a constant rotation of about 1000 rpm, the tilt of the body is slowed down due to the gyroscopic effect. The precession force acts on the horizontal axes of the gimbal. The Tilt Vs Time graph 'Figure 16' shows that the tilt starts at about 1.6 seconds and reaches 0° at 2.3 seconds (approximate value).

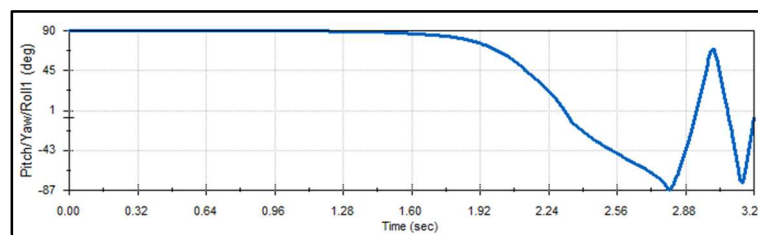


Figure 16. Tilt vs Time (1000 rpm)

5.2.3. Case 3: Flywheel at 3000 rpm. The maximum rpm of the motor, chosen for fabrication, is 3000rpm and the result of the Tilt vs Time graph 'Figure 17' was found for the same. The result shows that the greater the rpm of the flywheel, the longer it takes the body to tilt to 0°.

In the simulation, even after the 3.2-second mark, the body has tilted only about 32°.

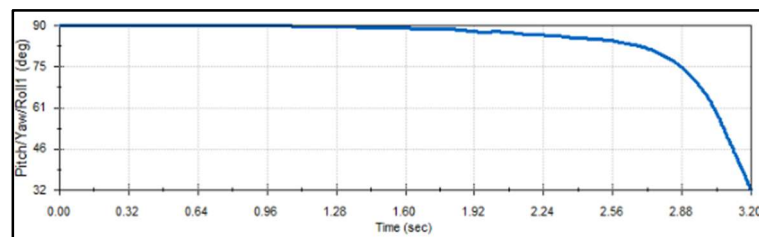


Figure 17. Tilt vs Time (3000 rpm)

5.2.4. *Analysis Result.* The dynamic analysis results are shown in 'Table 5'.

Table 5. Dynamic Analysis Result

Sl. No	RPM	Tilt Angle	Time taken
1	0	0-90	1.28
2	1000	0-90	2.30
3	3000	0-90	3.20

6. Conclusion

The result attained from the dynamic analysis shows that the time taken for the bicycle model to completely topple (0 to 90 degrees) increases with an increase in rpm of the flywheel and thus shows that the effect of precession increases with an increase in rpm and the weight of the flywheel. Further, the static analysis result reconfirms the appropriate material selection and the ability of each component to withstand the foresighted loads to manufacture efficiently. Thus, this study proves that the use of a gyroscope as an actuator can and is a plausible method of making a self-balancing bicycle and is far more stable and less prone to accidental tilts and toppling than one without a gyroscope. This prototype can be manufactured and the data studied can be used for further research.

References

- [1] Taraknath Taraphdar, Wasil Rasool Sheikh and Sourav Kumar 2014 Motorized Two Wheeler Accidents Caused by Animals: A Study *ISEMT-2014* 103
- [2] George Yannis, Constantinos Antoniou, Petros Evgenikos, Panagiotis Papantoniou, and Alan Kirk 2012 Characteristics and Causes of Power Two Wheeler Accidents in Europe *Procedia-Social and Behavioral Sciences* **48** 1535-44
- [3] https://en.wikipedia.org/wiki/Physical_disability
- [4] N. Tamaldin, H.I.M. Yusof, M.F.B. Abdollah, G. Omar, and M.I.F. Rosley 2017 Design self-balancing bicycle *MERD'17* 160-161
- [5] Qusai Suwan, Shirine El Zaatari, and Kareem Kassem 2017 Design and Evaluation of an Autonomous Self-balancing Bicycle *16th FEASAC*
- [6] https://en.wikipedia.org/wiki/Control_moment_gyroscope
- [7] Hemashree Kakar 2018 Design Calculations Of A Two Wheeler Self Balanced Vehicle *IRJET* **5** 2066-75
- [8] <https://global.yamaha-motor.com/about/design/concept/motoroid/>
<https://www.bmw-motorrad.com/en/experience/stories/brand/vision-next-100.html>
- [9] Md. Ashraful Alam, Vikram Yadama, William F. Cofer and Karl R. Englund 2012 Analysis and evaluation of a fruit bin for apples *J Food Sci Technol-2012*